Delayed Marrow Infusion in Mice Enhances Hematopoietic and Osteopoietic Engraftment by Facilitating Transient Expansion of the Osteoblastic Niche

Roberta Marino [1,†], Satoru Otsuru [1], Ted J. Hofmann [1], Timothy S. Olson [1], Valeria Rasini [2], Elena Veronesi [2], Kelli Boyd [3], Mostafa Waleed Gaber [4], Caridad Martinez [4], Paolo Paolucci [5], Massimo Dominici [2], Edwin M. Horwitz [1,*]

[1] Division of Oncology/Blood and Marrow Transplantation, Children's Hospital of Philadelphia and University of Pennsylvania School of Medicine, Philadelphia, Pennsylvania
[2] Department of Oncology, Hematology, and Respiratory Diseases, University-Hospital of Modena and Reggio Emilia, Modena, Italy
[3] Department of Pathology, Vanderbilt University School of Medicine, Nashville, Tennessee
[4] Department of Pediatrics, Baylor College of Medicine and Texas Children's Hospital, Houston, Texas
[5] Department of Mother and Child, University-Hospital of Modena and Reggio Emilia, Modena, Italy

ABSTRACT

Transplantation of bone marrow cells leads to engraftment of osteopoietic and hematopoietic progenitors. We sought to determine whether the recently described transient expansion of the host osteoblastic niche after marrow radioablation promotes engraftment of both osteopoietic and hematopoietic progenitor cells. Mice infused with marrow cells 24 hours after total body irradiation (TBI) demonstrated significantly greater osteopoietic and hematopoietic progenitor chimerism than did mice infused at 30 minutes or 6 hours. Irradiated mice with a lead shield over 1 hind limb showed greater hematopoietic chimerism in the irradiated limb than in the shielded limb at both the 6- and 24-hour intervals. By contrast, the osteopoietic chimerism was essentially equal in the 2 limbs at each of these intervals, although it significantly increased when cells were infused 24 hours compared with 6 hours after TBI. Similarly, the number of donor phenotypic long-term hematopoietic stem cells was equivalent in the irradiated and shielded limbs after each irradiation-to-infusion interval but was significantly increased at the 24-hour interval. Our findings indicate that a 24-hour delay in marrow cell infusion after TBI facilitates expansion of the endosteal osteoblastic niche, leading to enhanced osteopoietic and hematopoietic engraftment.

© 2013 Published by Elsevier Inc. on behalf of American Society for Blood and Marrow Transplantation.

INTRODUCTION

Transplantation of heterogeneous populations of bone marrow cells into radioablated hosts leads to engraftment of rare hematopoietic stem cells (HSCs) in the appropriate marrow niches in animal models and, presumably, in humans [1,2]. We [3-8] and others [9-12] have shown that transplantation of these marrow cells also leads to engraftment and differentiation of donor osteopoietic stem/progenitor cells. Osteopoietic donor chimerism is robust early after transplantation but decreases over time [7]. Nonetheless, the transplantable cells that give rise to osteopoiesis are capable of expansion in primary recipients and of engraftment and differentiation in secondary recipients, consistent with stem cell—like behavior [7].

Hematopoietic cells initially engraft at discrete sites in the epiphysis and metaphysis after bone marrow transplantation (BMT) [13-15], whereas donor-derived osteopoiesis invariably mirrors the locales of donor hematopoietic engraftment [7,13]. This suggests common niches for both regenerating activities, although direct support for this hypothesis is lacking.

Our observation that osteoblastic niches expand rapidly after marrow radioablation [13] led us to consider that the proliferating osteoblasts may support osteopoietic differentiation of the transplanted marrow cells. Here we report that transient expansion of host osteoblastic niches after marrow radioablation fosters the engraftment and differentiation of donor osteoprogenitors and that primitive hematopoietic progenitors engraft more readily in this expanded microenvironment. In this murine model, a 24-hour interval between radioablation and infusion of marrow cells facilitated engraftment of both osteopoietic and hematopoietic progenitors.

METHODS

Irradiation and BMT

Six- to 8-week-old FVB/N mice (Jackson Laboratory, Bar Harbor, ME) were given a lethal dose (1125 cGy, single dose) of total body irradiation (TBI) with a ^{137}Cs source (Gammacell 40 Exactor Irradiator; Nordion, Ottawa, Ontario, Canada) and were then transplanted with bone marrow cells obtained from 6- to 8-week-old enhanced green fluorescent protein (eGFP) transgenic FVB/N mice [7,16]. To study mice irradiated with single-leg shielding, we anesthetized the animals with a combination of ketamine (100 mg/kg i.p.) and xylazine (10 mg/kg i.p.), and then immobilized them on a flat support surface. The left hind limb was inserted into an apparatus with 3-cm lead plates blocking all radiation to that limb. At 30 minutes or at 6 or 24 hours after irradiation, the mice were injected with 2×10^6 eGFP$^+$ transgenic bone marrow cells. Unless otherwise noted, they were killed 3 weeks post-transplantation for flow cytometric analysis and/or immunohistochemical analysis. For flow cytometric analysis of hematopoietic stem/progenitor cells, marrow cells were obtained from the femoral

metaphyses. All animal protocols were approved by the Institutional Animal Care and Use Committees at the participating institutions.

Immunohistochemical Staining and Microscopy

Tissue processing and immunohistochemical staining for GFP to identify donor-derived bone cells were performed as previously described [13]. Briefly, bones were fixed in formalin and then decalcified with RegularCal•Immuno (BBC Biochemical Corporation, Mount Vernon, WA) and embedded in paraffin. Sections 6 μm thick were deparaffinized, rehydrated, and treated with Chondroitinase ABC solution (.35 IU/mL; Sigma-Aldrich, St. Louis, MO) at room temperature for 40 minutes for antigen retrieval. Sections were blocked with .1 M maleic buffer (Sigma-Aldrich) containing .15 M NaCl (Sigma-Aldrich), 2% blocking reagent (Roche Diagnostics GmbH, Mannheim, Germany), and 20% FCS (Gemini Bio-Products, West Sacramento, CA). Endogenous avidin and biotin were quenched using the Avidin/Biotin Blocking Kit (Vector Laboratories, Burlingame, CA). Sections were then incubated with rabbit anti-GFP antibody (1:250, Invitrogen, Carlsbad, CA) at 4°C overnight.

The following day, sections were incubated with biotinylated goat anti-rabbit antibody (1:200, Vector Laboratories) at room temperature for 1 hour followed by incubation for an hour with VECTASTAIN Elite ABC Reagent (Vector Laboratories). Color was developed using the NovaRED Substrate Kit (Vector Laboratories). The osteoblasts were identified as the large, cuboidal cells with eccentrically placed nuclei along the endosteal surface. Osteocytes were identified as single, often stellate-shaped, cells within the lacunae of bone. GFP$^+$ osteoblasts and osteocytes were enumerated using an AxioImager.A1 microscope equipped with an AxioCam HRc digital camera (Carl Zeiss MicroImaging, Inc., Thornwood, NY) by 2 investigators who were blinded to the experimental conditions.

Osteopoietic chimerism was determined as the percentage of GFP$^+$ bone cells in the epiphysis and metaphysis sampling a minimum of 200 cells per histologic section. The mean of 3 sections was taken as the chimerism for 1 animal. In an effort to eliminate experimental bias, we assessed osteopoietic chimerism throughout these studies with the microscopic evaluation of immunostained histologic sections because it is the most precise method to assess GFP$^+$ bone cells [17] and eliminates sampling errors.

Flow Cytometry

Bone marrow cells from the epiphysis and metaphysis of each femur were stained with the following antibodies: APC-conjugated anti-CD48, APC-Alexa Fluor 750 conjugated anti-c-Kit, PE-conjugated anti-CD150, PE-Cy5.5 conjugated anti-Sca-1 (eBioscience, San Diego, CA), and PE-Cy7 conjugated anti-Lineage (ie, CD4, CD8, CD11 b, Gr-1, B220, and Ter119; BD Biosciences, San Jose, CA). Flow cytometric analyses were performed on a FACSAria (BD Biosciences). Analysis of recipient marrow cells was restricted to the epiphysis and metaphysis of each femur because this is a site of early hematopoietic marrow engraftment [13-15] and osteopoietic engraftment [7,13].

Statistical Methods

All data are presented as means ± standard deviations. Statistical comparisons with a 2-tailed Student's t-test or with a 1-way analysis of variance with Tukey's multiple comparison test were considered significant if the differences attained $P \leq .05$. All analyses were performed with Prism software, version 4 (GraphPad Inc., San Diego, CA). To quantify the expansion of osteoblastic niches, we relied on a proliferation index based on the number of osteoblast layers along the endosteal surface: 1 = a single layer, 2 = 2 layers, 3 = 3 layers, and 4 = 4 or more layers.

RESULTS

Transplanted Donor Osteoprogenitors Engraft Within the Expanding Population of Endosteal Osteoblasts

We previously reported that the magnitude of donor-derived osteopoiesis is greatest early after BMT and decreases over the ensuing months [7]. Recognizing the abundance of endosteal osteoblasts comprising the niche expansion observed 48 hours after marrow radioablation [13], we reasoned that the transiently proliferating endosteal osteoblasts may create a permissive environment for osteopoietic differentiation. To begin to investigate mechanisms of donor osteoprogenitor engraftment, we assessed the kinetics of endosteal osteoblast proliferation during the first 72 hours after TBI (Figure 1A) using a proliferation index in which 1 represents a single layer of osteoblasts along the endosteal surface, 2 represents 2 layers, 3 represents 3 layers, and 4 represents 4 or more layers. Six hours after TBI, endosteal osteoblasts appeared mostly as a single layer. However, 48 hours after TBI, endosteal osteoblasts were more often observed in 3 or more layers (Figure 1A). The population of endosteal osteoblasts achieved the greatest observed rate of increase at 3 to 24 hours postirradiation (average rate, .080
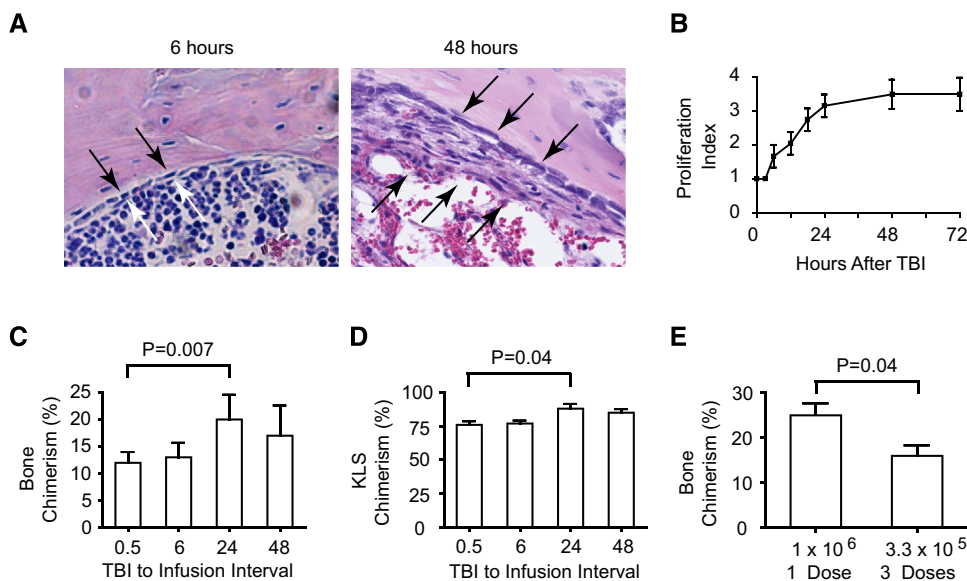
Figure 1. Kinetics of osteoblast proliferation and osteopoietic/hematopoietic chimerism. (A) Representative photomicrographs from 6 hours (left) and 48 hours (right) after TBI depicting the proliferation of the endosteal osteoblasts (arrows). (B) Time course of endosteal osteoblast proliferation in the metaphysis after TBI. Proliferation index as described in the text. Data points represent mean ± standard deviation. (C) Bone chimerism by time to cell infusion. Chimerism was defined as the fraction of GFP$^+$ osteoblasts and osteocytes in the metaphysis and epiphysis, determined by immunohistochemical staining and microscopic evaluation. (D) Chimerism within the KLS subpopulation of marrow cells according to the intervals from TBI to cell infusion, as determined by multicolor flow cytometric analysis of marrow isolated from transplanted mice. (E) Bone chimerism, determined as in (C), after different marrow dosing schedules. Bars represent mean ± standard deviation values.

units/hour), at which time approximately 90% of the maximal proliferation was attained. The rate then slowed (average rate, .014 units/hour) as the population of endosteal osteoblasts expanded to its maximum by 48 hours after TBI and then was stable at 72 hours (Figure 1B). Using BrdU and Ki-67 double-labeling experiments, we previously demonstrated that this expansion of the endosteal osteoblast population is due to proliferation of resident osteoblasts [18]. To determine if osteopoietic or hematopoietic engraftment was associated with the proliferative state of the endosteal osteoblasts, we transplanted bone marrow cells harvested from a transgenic GFP donor into lethally irradiated FVB/N mice at graded time intervals, from 30 minutes to 48 hours, after irradiation (5 mice per group). Three weeks after transplantation, the mice were killed and the femora were analyzed by immunohistochemical staining for donor (GFP$^+$) osteopoietic engraftment.

Marrow cells transplanted 30 minutes after TBI generated only 12.0% $\pm$ 2.0% osteopoietic engraftment (Figure 1C), similar to the result when marrow was infused 6 hours after TBI (13.0% $\pm$ 2.7%). By contrast, when marrow was infused 24 hours after irradiation, osteopoietic engraftment was significantly higher (20.0% $\pm$ 4.6% versus 12.0% $\pm$ 2.0%, $P = .007$); this finding was essentially unchanged at the 48-hour interval (17.0% $\pm$ 5.6%, $P =$ NS compared with 24 hours). There were no differences in the donor contribution to the short-term engraftment of unfractionated bone marrow, peripheral blood leukocytes, or Gr-1$^+$ neutrophils (data not shown); however, the c-Kit$^+$ lineage$^-$ Sca-1$^+$ (KLS) fraction of bone marrow, which represents primitive hematopoietic progenitors, showed significantly greater donor chimerism at this 3-week post-transplantation time point when cells were infused 24 hours rather than 30 minutes after irradiation (88.1% $\pm$ 8.1% versus 76.5% $\pm$ 6.2%, $P = .04$; Figure 1D).

We previously reported that the measured engraftment of donor osteopoietic cells after transplantation is saturable, indicating discrete engraftment sites [1]; that the endosteal osteoblast expansion after TBI correlates with expansion of cells characteristic of the stem cell niche [13] and with HSC engraftment [18], and that the osteoblast expansion is readily reversible after engraftment of transplanted hematopoietic cells [13], which seems to be driven specifically by engraftment of primitive hematopoietic progenitors [19]. Collectively, these data led us to consider that submaximal engraftment of transplantable osteopoietic progenitors may be associated with a reduction in the number of engraftment sites.

To test this hypothesis, we infused 9 mice with 1×10^6 marrow cells 24 hours after TBI and another 9 with 3 daily doses of 3.3×10^5 marrow cells (equal total cell dose in each group), beginning 24 hours after irradiation. Over this 24- to 72-hour interval, the magnitude of the osteoblast expansion remained stable (Figure 1B), suggesting the number of engraftment sites is stable [13] and the osteopoietic chimerism resulting from these 2 infusion protocols is similar. In contrast to this prediction, the osteopoietic chimerism produced by a single dose of 1×10^6 cells was significantly greater than that seen after the 3-dose regimen (25% $\pm$ 8% versus 16% $\pm$ 7%, $P = .04$, Figure 1E). These data suggest that the submaximal engraftment of donor osteoprogenitors after the first of the 3 doses may have down-regulated the total number of engraftment sites, thereby reducing the number of available sites for the transplantable osteoprogenitor and diminishing the osteopoietic engraftment potential of the 2 subsequent marrow cell doses.

Osteopoietic Engraftment without Direct Marrow Radioablation

To test the hypothesis that proliferating host osteoblasts are permissive for donor osteoprogenitor engraftment, we irradiated mice using a lead shield over the left hind limb. This enabled us to deliver 1125 cGy to the remainder of the body, including the lymphoid organs (to prevent rejection of the infused GFP-expressing cells), while the shielded hind limb remained protected, providing an internal control for assessing the effect of radioablation and niche expansion on osteoprogenitor engraftment.

Infusion of bone marrow cells 6 hours after TBI led to greater short-term donor chimerism in the irradiated leg compared with the shielded leg, whether total marrow cells (84% $\pm$ 3.6% versus 10% $\pm$ 2.6%, $P < .001$, n = 10) or KLS cells (71% $\pm$ 11.6% versus 3% $\pm$ .9%, $P < .001$, n = 10) (Figure 2A) were analyzed. Unexpectedly, osteopoietic engraftment was comparable in both hind legs (15% $\pm$ 4.0% versus 17% $\pm$ 1.5%) at this interval (Figure 2A). Similar results were obtained when the marrow cells were infused 24 hours after TBI (Figure 2B). Control mice, which were irradiated without leg shielding, showed similar hematopoietic and osteopoietic chimerism values in the 2 legs when marrow was infused either 6 or 24 hours after TBI (Figure 2C,D).

Early versus Late Marrow Transplantation

Our data indicate that transplanting marrow cells 24 hours after TBI leads to greater hematopoietic progenitor and osteopoietic engraftment than cells transplanted after a shorter interval (Figure 1), possibly because of radioablation-induced expansion of host osteoblastic niches. However, osteopoietic engraftment, in contrast to hematopoietic engraftment, seems to be similar with or without marrow radioablation (Figure 2). In an effort to understand this incongruity, we compared chimerism results for each leg, irradiated and shielded, independently of the other. When marrow was infused 24 hours after TBI, compared with 6 hours, the irradiated leg displayed a significant decrease in both total marrow chimerism (84% $\pm$ 3.6% versus 40% $\pm$ 18.9%, $P < .001$) and hematopoietic progenitor (KLS cell) chimerism (71% $\pm$ 11.6% versus 53% $\pm$ 19.1%, $P = .04$) (Figure 3A). Osteopoietic chimerism, by contrast, was clearly greater in mice infused after the longer interval (37.4% $\pm$ 12.9% versus 17.0% $\pm$ 1.5%, $P = .009$, Figure 3A), consistent with the notion that delay between TBI and marrow infusion promotes host osteoblast proliferation, thereby facilitating donor osteopoietic engraftment.

Comparison of data for the shielded leg at both intervals revealed comparable total marrow chimerism values (10.5% $\pm$ 2.6% versus 12.1% $\pm$ 3.1%), but, notably, the KLS chimerism was 2-fold greater after marrow infusion at 24 hours (2.6% $\pm$ .9% versus 5.3% $\pm$ 2.5%, $P = .04$; Figure 3B). Similar to results for the irradiated leg, osteopoietic chimerism was significantly increased at the 24- compared with the 6-hour interval (15.4% $\pm$ 3.9% versus 30.1% $\pm$ 12.1%, $P = .02$, Figure 3B).
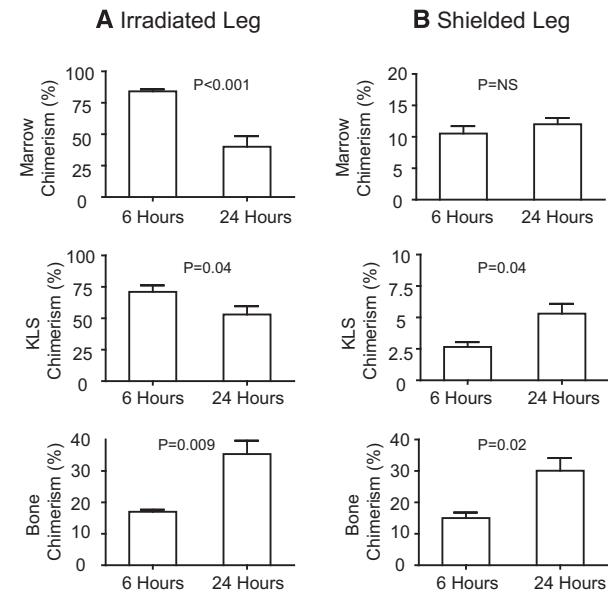
HSC Engraftment

Engraftment of primitive osteoprogenitors is greater when donor cells are infused 24 hours rather than 6 hours after TBI, even when the marrow space is shielded from radiation (Figure 3B). To address whether this relationship extends to HSCs, we analyzed the engrafted hematopoietic marrow cells for the surface phenotype of CD150$^+$ CD48$^-$ CD41$^-$ (designated SLAM cells) after transplantation. First
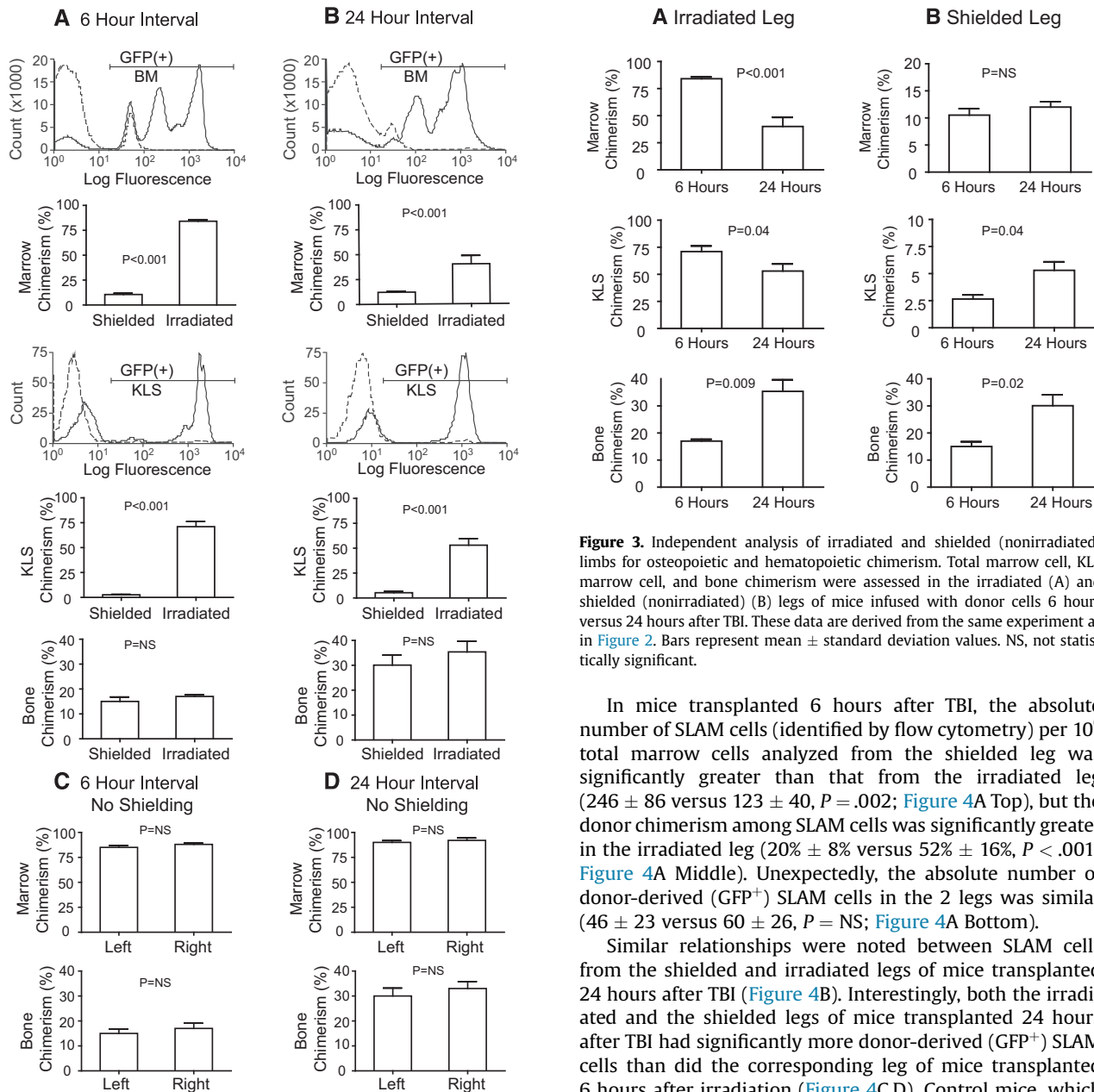
Figure 2. Comparison of osteopoietic and hematopoietic chimerism in irradiated versus shielded (nonirradiated) limbs according to time from TBI to marrow infusion. Total marrow cell, KLS marrow cell, and bone chimerism were determined in shielded versus irradiated legs 3 weeks posttransplantation, when donor cells were transplanted at (A) 6 hours or (B) 24 hours. Histograms are representative of the flow cytometric analyses for the bone marrow and KLS chimerism in shielded (- - -) and unshielded (—) legs. Total marrow cell and bone chimerism were determined in left and right legs (both unshielded during irradiation) of control mice 3 weeks posttransplantation, when donor cells were transplanted at (C) 6 hours or (D) 24 hours. In all graphs, bars represent the mean ± standard deviation (n = 10). NS, not statistically significant.

Figure 3. Independent analysis of irradiated and shielded (nonirradiated) limbs for osteopoietic and hematopoietic chimerism. Total marrow cell, KLS marrow cell, and bone chimerism were assessed in the irradiated (A) and shielded (nonirradiated) (B) legs of mice infused with donor cells 6 hours versus 24 hours after TBI. These data are derived from the same experiment as in Figure 2. Bars represent mean ± standard deviation values. NS, not statistically significant.

described by Kiel et al. [20], this phenotype distinguishes a primitive hematopoietic population enriched for long-term repopulating cells. In each experiment, mice were killed for analysis 3 weeks after TBI. Marrow cellularity, assessed by visual inspection of histologic sections, and the total number of recovered cells were similar between the shielded and irradiated limbs (data not shown).

In mice transplanted 6 hours after TBI, the absolute number of SLAM cells (identified by flow cytometry) per 10^6 total marrow cells analyzed from the shielded leg was significantly greater than that from the irradiated leg (246 ± 86 versus 123 ± 40, $P = .002$; Figure 4A Top), but the donor chimerism among SLAM cells was significantly greater in the irradiated leg ($20\% \pm 8\%$ versus $52\% \pm 16\%$, $P < .001$; Figure 4A Middle). Unexpectedly, the absolute number of donor-derived (GFP$^+$) SLAM cells in the 2 legs was similar (46 ± 23 versus 60 ± 26, $P =$ NS; Figure 4A Bottom).

Similar relationships were noted between SLAM cells from the shielded and irradiated legs of mice transplanted 24 hours after TBI (Figure 4B). Interestingly, both the irradiated and the shielded legs of mice transplanted 24 hours after TBI had significantly more donor-derived (GFP$^+$) SLAM cells than did the corresponding leg of mice transplanted 6 hours after irradiation (Figure 4C,D). Control mice, which received TBI without shielding (both legs irradiated), had equivalent absolute number of SLAM cells, SLAM chimerism, and absolute number of donor SLAM cells in both legs, documenting the lack of preferential engraftment in our model (data not shown).

Of interest, the overall number of SLAM cells per leg in the control mice was 860 ± 508, statistically indistinguishable from the finding in the irradiated leg (804 ± 264) but less than that in the shielded leg (1480 ± 720, $P = .04$) of the experimental mice. The chimerism in the control mice was $64.3\% \pm 8.2\%$, or 2-fold greater than results for the irradiated ($P < .001$) and shielded ($P < .001$) legs. Moreover, the absolute number of GFP$^+$ SLAM cells was 444 ± 264, greater than findings in either the irradiated ($P = .05$) or shielded legs ($P = .04$).

Osteoblast Niche Proliferation

In addition to the vital role of endosteal osteoblast expansion and marrow niche remodeling for HSC engraftment
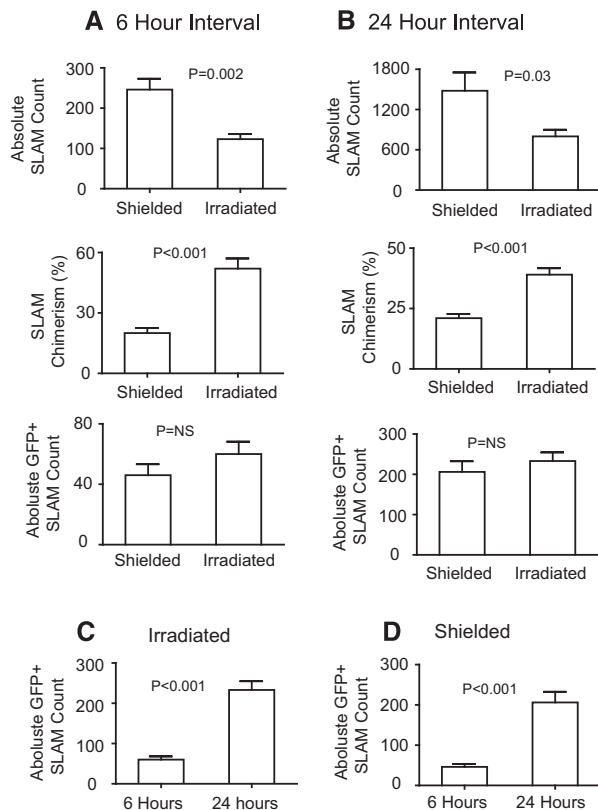
Figure 4. Engraftment of CD150^{+} CD48^{−} CD41^{−} (SLAM) cells in irradiated and shielded (nonirradiated) limbs. SLAM cells were measured in the bone marrow from the shielded or irradiated legs of mice transplanted at (A) 6 hours or (B) 24 hours after TBI and analyzed for chimerism and other engraftment parameters. The absolute SLAM count represents the number of SLAM cells per 10[6] viable marrow cells as determined by flow cytometry. Chimerism is the percentage of donor-derived (GFP^{+}) SLAM cells. The absolute GFP[+] SLAM count represents the number of GFP^{+} SLAM cells per 10[6] viable marrow cells. (C) Comparison of the absolute GFP[+] SLAM count in the irradiated limb when marrow was infused 6 hours versus 24 hours after TBI. (D) Comparison of the absolute GFP[+] SLAM count in the shielded (nonirradiated) limb when marrow was infused 6 hours versus 24 hours after TBI. In all panels, bars represent the mean ± standard deviation values. NS, not statistically significant.

[13,18,21], we postulated that osteoblastic niche expansion contributes to a permissive environment for osteoprogenitor engraftment and differentiation as well. To test this prediction in a rigorous manner, it was necessary to quantify the expansion of these niches. We therefore irradiated mice using our leg-shielding apparatus and then calculated the proliferation index as in Figure 1A,B.

Analysis of histologic sections of paired (shielded and irradiated) femora taken 24 hours after irradiation demonstrated substantial osteoblast proliferation in the irradiated leg (3.16 ± .3; Figure 5A,E), which was significantly greater than in the shielded leg (1.43 ± .5, $P < .001$; Figure 5B,E), as predicted by our previous study [13]. Although the proliferation index for osteoblasts in the shielded leg was low (1.43 ± .5), it did significantly exceed the index for nonirradiated controls (1.0 ± .0, n = 8, $P = .03$; Figure 5C,E). Interestingly, the shielded leg of the irradiated mice exhibited several areas of more cuboidal, or so-called plump, osteoblasts [22] (Figure 5D), which are commonly observed in the endosteal niche of radioablated marrow (Figure 5A), compared with the flattened appearance of these cells at homeostasis (Figure 5C), which one would expect in the absence of radioablation.

DISCUSSION

We previously reported donor-derived osteopoiesis after BMT in children with osteogenesis imperfecta [3], which was associated with measurable clinical benefit [4]. More recently, BMT has been reported to effectively ameliorate the osteogenesis imperfecta phenotype in a mouse model [12], corroborating our clinical investigation. We also demonstrated the osteopoietic differentiation potential of transplanted murine bone marrow cells [5,6]. Independent confirmation of this observation [9-12] has established the osteopoietic capacity of heterogeneous populations of transplanted marrow cells. Indeed, marrow cells hold promise as cell therapy for an array of bone disorders [23]. Our current data show that delaying marrow infusion for 24 hours after TBI leads to a significantly greater level of osteopoietic engraftment than can be achieved with earlier infusions. These findings suggest that transient expansion of host osteoblastic niches [13], which, in our FVB/N murine model, becomes near-maximal at 24 hours [17,18] (Figure 1B), may be a critical regulator of donor osteoprogenitor differentiation to osteoblasts.

Interestingly, 4-fold more HSCs, identified phenotypically as CD150^{+} CD48^{−} CD41^{−} [20], were found in the mice at 3 weeks post-transplantation when marrow was infused at 24 hours, compared with 6 hours, after TBI. Delaying marrow infusion after TBI has been shown to promote donor cell engraftment, as measured by hematopoietic reconstitution, and may be superior to infusion immediately after TBI [24-26]. These studies have generally attributed improved hematopoietic reconstitution after delayed marrow cell infusion to the partial clearance of proinflammatory cytokines that are released in response to TBI-induced host tissue damage and may be associated with the early events of graft-versus-host disease [27,28] and possibly graft rejection. Our data provide an intriguing alternative explanation: Transient expansion of the endosteal niche after radioablation fosters engraftment of both primitive hematopoietic cells and osteoprogenitors.

To assess the effect of radioablation-induced endosteal niche proliferation in a rigorously controlled manner, we shielded one hind limb during TBI to prevent niche expansion in a defined marrow region. As expected, the donor chimerism among all marrow cells and hematopoietic progenitors (KLS cells) was significantly greater in the irradiated limb compared with the shielded limb. Surprisingly, however, the percentages of osteopoietic chimerism in the 2 limbs did not differ appreciably, indicating that neither direct exposure of the bone to ionizing radiation nor marrow cell ablation is required for engraftment and differentiation of transplantable marrow osteoprogenitor cells. We also found it striking that the number of phenotypically defined donor HSCs (SLAM cells) was essentially identical in both limbs. Thus, ablation of host marrow cells does not appear to facilitate early engraftment of the transplanted donor HSCs. Although this observation may seem counterintuitive and, indeed, contradictory to the importance of osteoblast niche expansion for HSC engraftment, it is in fact consistent with our current understanding of stem cell niches and suggests an especially important role of niche remodeling for HSC engraftment.

Given that the 2 hind limbs (which in our experience contain about 60 × 10^{6} nucleated marrow cells) represent an estimated 25% of the total marrow volume of a mouse [29], the 2 × 10^{6} nucleated cell transplant used in this study accounted for less than 1% of the marrow cell compartment. Because roughly the same fraction of niches (∼1%) is
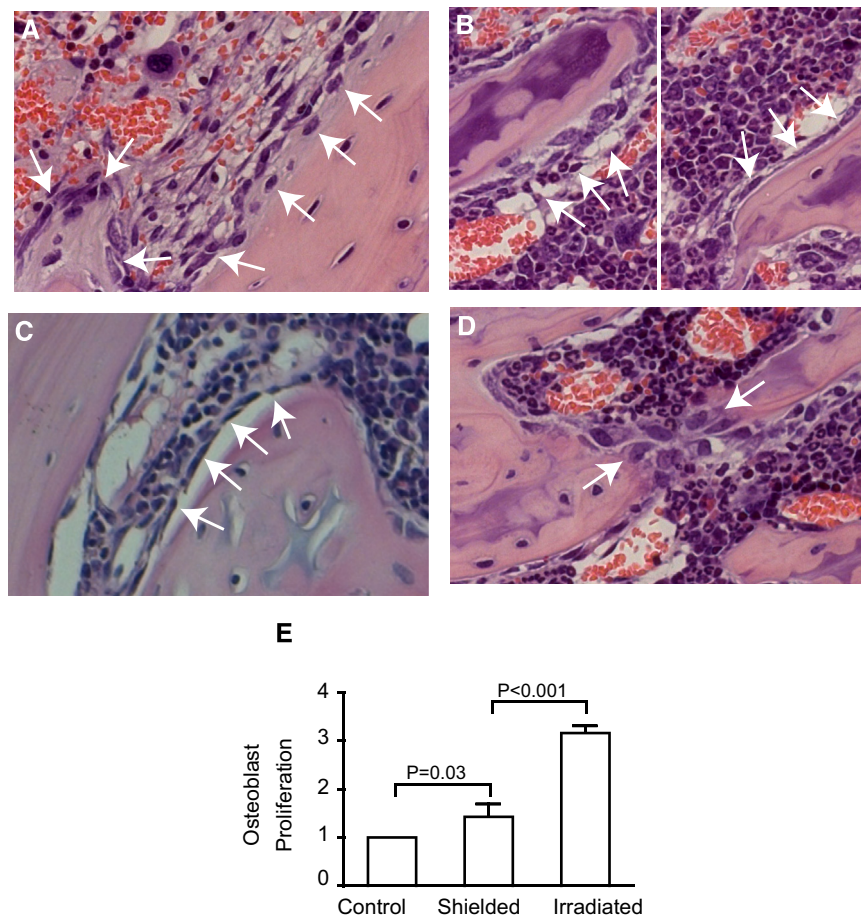
Figure 5. Endosteal osteoblast proliferation in the irradiated versus shielded (nonirradiated) limbs. The photomicrographs depict H & E staining of femora taken from mice 24 hours after TBI. (A) Femur section from an irradiated limb; arrows indicate osteoblasts. (B) Femur section from shielded limb depicting regions of proliferating osteoblasts (multiple cell layers, left) and quiescent osteoblasts (single cell layer, right). (C) Femur section from a control (nonirradiated) mouse included for comparison; arrows indicate osteoblasts. (D) Selected region of a femur from a shielded limb demonstrating so-called plump osteoblasts in contrast to the more flattened cells seen elsewhere in the shielded limb (B) or during homeostasis (C). (E) Comparison of the magnitude of osteoblast proliferation, scored according to the proliferation index (see Methods) among femora from nonirradiated mice (controls), shielded limbs from irradiated mice, and irradiated limbs. Data were analyzed using a 1-way analysis of variance with Tukey's multiple comparison test comparing each experimental group with the controls. The bars represent mean ± standard deviation.

thought to be unoccupied during homeostasis and therefore available for donor cell engraftment [30], we would argue that the transplanted cells were distributed equally throughout the host marrow space: in the irradiated, ablated hematopoietic marrow with most niches unoccupied and the shielded, intact hematopoietic marrow with homeostatic ~1% of the niches unoccupied. This interpretation implies that not only osteoblast expansion, which was observed in the shielded limb (Figure 5E), but other components of niche remodeling, including the morphologic changes of osteoblasts (Figure 5D) and megakaryocyte migration [13,21], may also effectively contribute to HSC engraftment. Moreover, ablation of a fraction of the host marrow may elicit the release of circulating factors that foster engraftment of transplanted donor HSCs throughout the marrow space. Thus, partial marrow radioablation may facilitate early engraftment of the transplanted donor HSCs, although direct ablation of the engrafting sites is not required. Finally, we cannot infer from our data whether the transplanted HSCs displaced host HSCs, although this outcome is thought to be highly unlikely [30].

The leg-shielding studies provided further biologic insight into HSC engraftment. In the shielded leg of the 6-hour infusion cohort, the chimerism of HSCs (defined as SLAM cells) was 20%, whereas that of the hematopoietic progenitor (KLS) cells was only 3% and that of the total marrow, 10%. A similar quantitative relationship was observed in the 24-hour cohort. These data indicate that not all donor HSCs engrafting in the shielded marrow space gave rise to hematopoietic cells early after engraftment, possibly because the microenvironmental cues needed to stimulate HSC proliferation and differentiation were lacking in the relatively well-populated nonirradiated marrow space. Indeed, when mice were assessed at 3 weeks post-transplantation, the relative magnitude of HSC chimerism more closely paralleled the osteopoietic chimerism rather than the hematopoietic progenitor or total marrow chimerism, which is reflected by blood chimerism. This may be due to a dual hematopoietic–osteopoietic differentiation capacity of the HSC early after BMT so that osteopoietic chimerism is derived from the HSC [5,6,10,12,31]. Hence, in murine models, osteopoietic engraftment assessed early after BMT (e.g., 2 to 3 weeks) may provide a more reliable index of HSC engraftment than does peripheral blood chimerism.

Another observation of interest is that the number of engrafted donor HSCs increased in the shielded leg

concomitant with decreases in the HSC, KLS, and total marrow chimerism in the irradiated leg of mice infused at 24 versus 6 hours postirradiation. Because HSCs are known to migrate to different areas of the bone marrow space [32,33], we suggest that some of the HSCs in the shielded leg had time to migrate to the ablated leg during the 24-hour interval between TBI and marrow cell infusion where they began to proliferate and repopulated the ablated marrow with host (GFP⁻) cells. Thus, the engrafted donor cells accounted for a smaller percentage (reduced chimerism) of the repopulated marrow space.

In shielded legs, the osteoblast proliferation, albeit low, was greater than in negative controls, with some osteoblasts demonstrating a plump morphology (Figure 5D) similar to that commonly observed after radioablation [13]. This morphologic change alters the biomechanical properties of the osteoblast governing adhesion, which may foster greater HSC engraftment than would be predicted from the osteoblast proliferation alone [34]. These observations suggest novel cross-talk in the osteoblastic niche, instigated when niche disruption by TBI signals the absence of occupying HSCs. In response, HSCs from the shielded leg might egress from their marrow niches into the circulation and home to available niches in the irradiated leg. This engraftment would be expected to quench niche signaling, thereby ending HSC migration. This notion gains support from our previous observation that the osteoblastic niche expansion seen after radioablation is readily reversed by primitive hematopoietic cell engraftment [13,18] and our current data showing that osteopoietic engraftment is decreased if small cell doses are transplanted on successive days, possibly due to down-regulation of the engrafting niches recognized by osteoprogenitors.

Finally, our data suggest a novel strategy of reduced-intensity marrow conditioning. With adequate immune suppression to prevent rejection (which was not a limiting factor in our studies because of the use of syngeneic inbred strains of mice), one could deliver ablative agents to selected nonvital structures such as the limbs and peripheral pelvis to achieve greater total donor cell engraftment than is commonly attained. Once engrafted, the donor cells would differentiate and expand to occupy the entire marrow space [32]. Our future efforts will be directed toward developing optimal transplantation strategies for both hematopoietic and osteopoietic engraftment. We anticipate that the microenvironmental changes we previously identified [13] will play a pivotal role in understanding the mechanisms of stem cell engraftment and osteopoietic differentiation and thus in successfully meeting this challenge.

ACKNOWLEDGMENTS

REFERENCES

1. Marino R, Martinez C, Boyd K, et al. Transplantable marrow osteoprogenitors engraft in discrete saturable sites in the marrow microenvironment. *Exp Hematol.* 2008;36:360-368.
2. Andrade J, Ge S, Symbatyan G, et al. Effects of sublethal irradiation on patterns of engraftment after murine bone marrow transplantation. *Biol Blood Marrow Transplant.* 2011;17:608-619.
3. Horwitz EM, Prockop DJ, Fitzpatrick LA, et al. Transplantability and therapeutic effects of bone marrow-derived mesenchymal cells in children with osteogenesis imperfecta. *Nat Med.* 1999;5:309-313.
4. Horwitz EM, Prockop DJ, Gordon PL, et al. Clinical responses to bone marrow transplantation in children with severe osteogenesis imperfecta. *Blood.* 2001;97:1227-1231.
5. Dominici M, Pritchard C, Garlits JE, et al. Hematopoietic cells and osteoblasts are derived from a common marrow progenitor after bone marrow transplantation. *Proc Natl Acad Sci USA.* 2004;101:11761-11766.
6. Hofmann TJ, Otsuru S, Marino R, et al. Transplanted murine long-term repopulating hematopoietic cells can differentiate to osteoblasts in the marrow stem cell niche. *Mol Ther.* 2013;21:1224-1231.
7. Dominici M, Marino R, Rasini V, et al. Donor cell-derived osteopoiesis originates from a self-renewing stem cell with a limited regenerative contribution after transplantation. *Blood.* 2008;111:4386-4391.
8. Otsuru S, Gordon PL, Shimono K, et al. Transplanted bone marrow mononuclear cells and MSCs impart clinical benefit to children with osteogenesis imperfecta through different mechanisms. *Blood.* 2012; 120:1933-1941.
9. Nilsson SK, Dooner MS, Weier HU, et al. Cells capable of bone production engraft from whole bone marrow transplants in nonablated mice. *J Exp Med.* 1999;189:729-734.
10. Olmsted-Davis EA, Gugala Z, Camargo F, et al. Primitive adult hematopoietic stem cells can function as osteoblast precursors. *Proc Natl Acad Sci USA.* 2003;100:15877-15882.
11. Wang L, Liu Y, Kalajzic Z, et al. Heterogeneity of engrafted bone-lining cells after systemic and local transplantation. *Blood.* 2005;106:3650-3657.
12. Mehrotra M, Rosol M, Ogawa M, Larue AC. Amelioration of a mouse model of osteogenesis imperfecta with hematopoietic stem cell transplantation: microcomputed tomography studies. *Exp Hematol.* 2010;38:593-602.
13. Dominici M, Rasini V, Bussolari R, et al. Restoration and reversible expansion of the osteoblastic hematopoietic stem cell niche after marrow radioablation. *Blood.* 2009;114:2333-2343.
14. Askenasy N, Zorina T, Farkas DL, Shalit I. Transplanted hematopoietic cells seed in clusters in recipient bone marrow in vivo. *Stem Cells.* 2002; 20:301-310.
15. Askenasy N, Stein J, Yaniv I, Farkas DL. The topologic and chronologic patterns of hematopoietic cell seeding in host femoral bone marrow after transplantation. *Biol Blood Marrow Transplant.* 2003;9:496-504.
16. Dominici M, Tadjali M, Kepes S, et al. Transgenic mice with pancellular enhanced green fluorescent protein expression in primitive hematopoietic cells and all blood cell progeny. *Genesis.* 2005;42:17-22.
17. Otsuru S, Hofmann TJ, Rasini V, et al. Osteopoietic engraftment after bone marrow transplantation: effect of inbred strain of mice. *Exp Hematol.* 2010;38:836-844.
18. Caselli A, Olson TS, Otsuru S, et al. IGF-1-mediated osteoblastic niche expansion enhances long-term hematopoietic stem cell engraftment after murine bone marrow transplantation. *Stem Cells.* 2013. http://dx.doi.org/10.1002/stem.1463. [Epub ahead of print].
19. Essers MA, Trumpp A. Targeting leukemic stem cells by breaking their dormancy. *Mol Oncol.* 2010;4:443-450.
20. Kiel MJ, Yilmaz OH, Iwashita T, et al. SLAM family receptors distinguish hematopoietic stem and progenitor cells and reveal endothelial niches for stem cells. *Cell.* 2005;121:1109-1121.
21. Olson TS, Caselli A, Otsuru S, et al. Megakaryocytes promote murine osteoblastic HSC niche expansion and stem cell engraftment after radioablative conditioning. *Blood.* 2013;121:5238-5249.
22. Katayama Y, Battista M, Kao WM, et al. Signals from the sympathetic nervous system regulate hematopoietic stem cell egress from bone marrow. *Cell.* 2006;124:407-421.
23. Jethva R, Otsuru S, Dominici M, Horwitz EM. Cell therapy for disorders of bone. *Cytotherapy.* 2009;11:3-17.
24. Ding Y, Rotta M, Graves SS, et al. Delaying DLA-haploidentical hematopoietic cell transplantation after total body irradiation. *Biol Blood Marrow Transplant.* 2009;15:1244-1250.
25. Lichter AS, Tracy D, Lam WC, Order SE. Total body irradiation in bone marrow transplantation: the influence of fractionation and delay of marrow infusion. *Int J Radiat Oncol Biol Phys.* 1980;6:301-309.
26. Weiss L, Bullorsky E, Ashkenazi YJ, Slavin S. Optimal time interval between myeloablative whole body irradiation and reconstitution with syngeneic bone marrow graft. *Bone Marrow Transplant.* 1988;3: 207-210.
27. Antin JH, Ferrara JL. Cytokine dysregulation and acute graft-versus-host disease. *Blood.* 1992;80:2964-2968.
28. Reddy P, Ferrara JL. Immunobiology of acute graft-versus-host disease. *Blood Rev.* 2003;17:187-194.
29. Boggs DR. The total marrow mass of the mouse: a simplified method of measurement. *Am J Hematol.* 1984;16:277-286.
30. Bhattacharya D, Rossi DJ, Bryder D, Weissman IL. Purified hematopoietic stem cell engraftment of rare niches corrects severe lymphoid deficiencies without host conditioning. *J Exp Med.* 2006;203:73-85.

31. Mehrotra M, Williams CR, Ogawa M, LaRue AC. Hematopoietic stem cells give rise to osteochondrogenic cells. *Blood Cells Mol Dis*. 2013;50: 41-49.

32. Ito H, Takeuchi Y, Shaffer J, Sykes M. Local irradiation enhances congenic donor pluripotent hematopoietic stem cell engraftment similarly in irradiated and nonirradiated sites. *Blood*. 2004;103: 1949-1954.

33. Dar A, Kollet O, Lapidot T. Mutual, reciprocal SDF-1/CXCR4 interactions between hematopoietic and bone marrow stromal cells regulate human stem cell migration and development in NOD/SCID chimeric mice. *Exp Hematol*. 2006;34:967-975.

34. Lee-Thedieck C, Rauch N, Fiammengo R, et al. Impact of substrate elasticity on human hematopoietic stem and progenitor cell adhesion and motility. *J Cell Sci*. 2012;5(Pt 16):3765-3775.